Acta Cryst. (1973). A**29**, 192

The Theory of X-ray Crystal Diffraction for Finite Polyhedral Crystals. III. The Bragg–(Bragg)^m Cases

BY T. SAKA, T. KATAGAWA AND N. KATO

Department of Applied Physics, Faculty of Engineering, Nagoya University, Nagoya, Japan

(*Received* 17 *April* 1972; *accepted* 31 *October* 1972)

The plane-wave and spherical-wave theories are described for the Bragg–(Bragg)^m cases. The treatment is similar to that of Parts I and II [Saka, Katagawa & Kato (1972). *Acta Cryst.* A**28**, 102–113, 113–120] for the Laue–(Bragg)^m cases. In the plane-wave theory of the Bragg case, a few aspects which up to now have not been well understood, are described to clarify the mathematical structures of the wave field. In particular, emphasis is put on a method for specifying the plane-wave solution by using a Riemann sheet instead of the dispersion surface. In the spherical-wave theory, the reflected vacuum wave and the transmitted crystal wave at the entrance surface can be represented by two Bessel functions. The crystal wave of the Bragg–(Bragg)^m case reflected at the exit surface is represented by a combination of two Bessel functions. The transmitted vacuum wave, however, is given by a combination of four Bessel functions. It is shown that the solutions are compatible with those of the Laue–(Bragg)^m cases. The solution for finite polyhedral crystals can be constructed by superposing the solutions for individual cases such as of Laue, Laue–(Bragg)^m [Kato (1968). *J. Appl. Phys.* **39**, 2225-2230; Parts I and II] and Bragg–(Bragg)^m obtained in the present paper. A comparison is made with Uragami's results obtained by another approach [*J. Phys. Soc. Japan* (1969), **27**, 147–154; (1970), **28**, 1508–1527].

1. Introduction

Following Parts I and II (Saka, Katagawa & Kato, 1972*a*, *b*), this Part treats X-ray diffraction for the crystals bounded by plane surfaces in an arbitrary way, but under the condition that the Bragg-reflected wave emerges from the entrance surface. Both the plane-wave and spherical-wave theories are formulated. The diffraction phenomena under this geometrical condition are specified by the Bragg–(Bragg)^m cases ($m=0,1,2,\ldots$) in the present terminology.

Traditionally, plane-wave theories have been developed for semi-infinite crystals or parallel-sided crystals (*e.g.*, Zachariasen, 1945). The rays associated with the wave fields were discussed by Wagner (1956). The present theory is an extension of these theories regarding the crystal form. The spherical wave treatments were developed by Uragami (1969, 1970) based on the dynamical theories of Takagi (1962, 1969) and Taupin (1964).* The present results are essentially equivalent to those of Uragami except for a constant factor, although the formulation is quite different. It is shown that the correct solution can be obtained in Uragami's formulation if one correctly takes into account the amplitude and phase of the incident wave.

According to the present general approach, the plane-wave solution is first formulated and then the spherical-wave solution is obtained by Fourier transformation of the plane-wave solution. The exact Fourier integrals required are obtained by the standard contour integral method. In order to justify the contour adopted, one needs to prove some mathematical structures of the plane-wave solution. These subjects were reported in a separate paper (Kato, Katagawa & Saka, 1971). The important results are summarized at the beginning of the next Section.†

Except for the details, the formulation for the Bragg–(Bragg)^m cases is surprisingly similar to that for the Laue–(Bragg)^m cases in both the plane-wave and spherical-wave theories. Combining the wave fields

* Recently, Afanas'ev & Kohn (1971) have also solved the problem for parallel-sided crystals using the Takagi–Taupin approach.

† Some of the results have also been obtained by Fingerland (1971) in a different form.

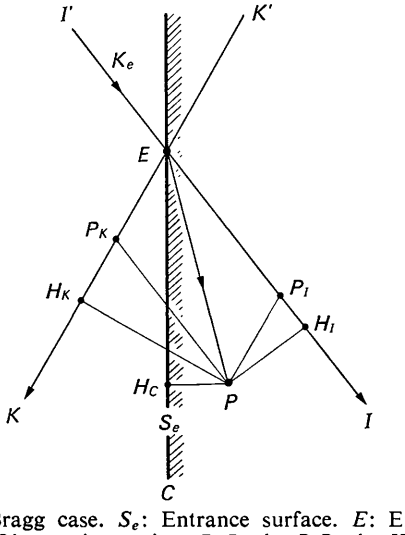

Fig. 1. The Bragg case. S_e: Entrance surface. E: Entrance point. P: Observation point. $P_KP=l_0$, $P_IP=l_g$, $H_IP=x_0$, $H_KP=x_g$. x_0 is positive when P is on the left side of II'. x_g is positive when P is on the right side of KK'. $H_CP=t=[\mathbf{n}_e\,.\,(\mathbf{r}-\mathbf{r}_e)]$: The depth of the observation point P from the surface S_e.

obtained in the present and previous papers (Kato, 1968; Parts I and II), one can construct the wave fields arising from diffraction for the crystals of any polyhedral shape.

In the following, equations, figures and tables of Parts I and II will be referred to by the Roman numbers I and II respectively. Often, the notations of the previous Parts will be used without further explanation.

2. The Bragg case

(*a*) *Plane-wave theory*

When an incident wave $E_e \exp[i(\mathbf{K}_e \cdot \mathbf{r})]$ falls on the entrance surface under the condition of the Bragg case (Fig. 1), the following waves are excited: the crystal waves:

$$d_0(\mathbf{r}) = E_e \exp\{i[(\mathbf{K}_e \cdot \mathbf{r}_e) + (\mathbf{k}_0 \cdot (\mathbf{r}-\mathbf{r}_e))]\} \quad (1a)$$

$$d_g(\mathbf{r}) = c \exp[2\pi i(\mathbf{g} \cdot \mathbf{r}_e)]\, E_e \exp\{i[(\mathbf{K}_e \cdot \mathbf{r}_e) + (\mathbf{k}_g \cdot (\mathbf{r}-\mathbf{r}_e))]\} \quad (1b)$$

the vacuum wave:

$$E_g(\mathbf{r}) = c \exp[2\pi i(\mathbf{g} \cdot \mathbf{r}_e)]\, E_e \exp\{i[(\mathbf{K}_e \cdot \mathbf{r}_e) + (\mathbf{K}_g \cdot (\mathbf{r}-\mathbf{r}_e))]\} \quad (1c)$$

where $\mathbf{k}_0$, $\mathbf{k}_g = \mathbf{k}_0 + 2\pi\mathbf{g}$ and $\mathbf{K}_g$ are the wave vectors of the relevant waves. As constructed in Fig. 2, they are connected with $\mathbf{K}_e$ through the tangential continuity on the entrance surface and, in terms of the deviation parameter s defined by equation (I.10) or K_x, x component of $\mathbf{K}_e$, given in the forms

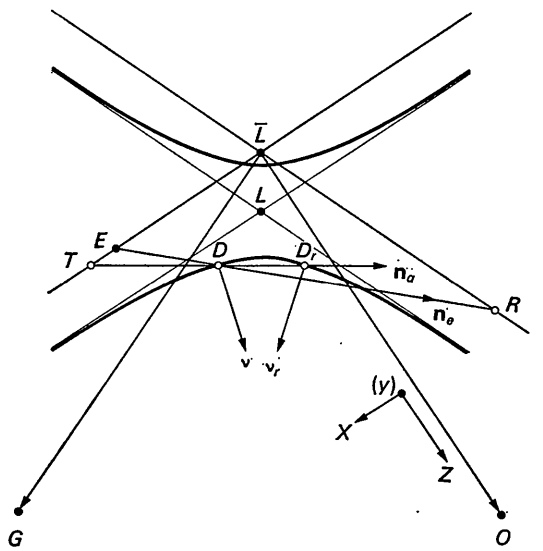

Fig. 2. The construction of the dispersion points (the Bragg and Bragg–Bragg cases). $\mathbf{n}_e$: The inward normal of the entrance surface S_e. $\mathbf{n}_a$: The outward normal of the exit surface S_a. $\vec{LO}=\bar{\mathbf{K}}_0$, $\vec{LO}=\mathbf{k}_0$, $\vec{EO}=\mathbf{K}_e$, $\vec{DO}=\mathbf{k}_0$, $\vec{D_rO}=\mathbf{k}_{0,r}$, $\vec{LG}=\bar{\mathbf{K}}_g$, $\vec{LG}=\bar{\mathbf{k}}_g$, $\vec{RG}=\mathbf{K}_g$, $\vec{DG}=\mathbf{k}_g$, $\vec{D_rG}=\mathbf{k}_{g,r}$.

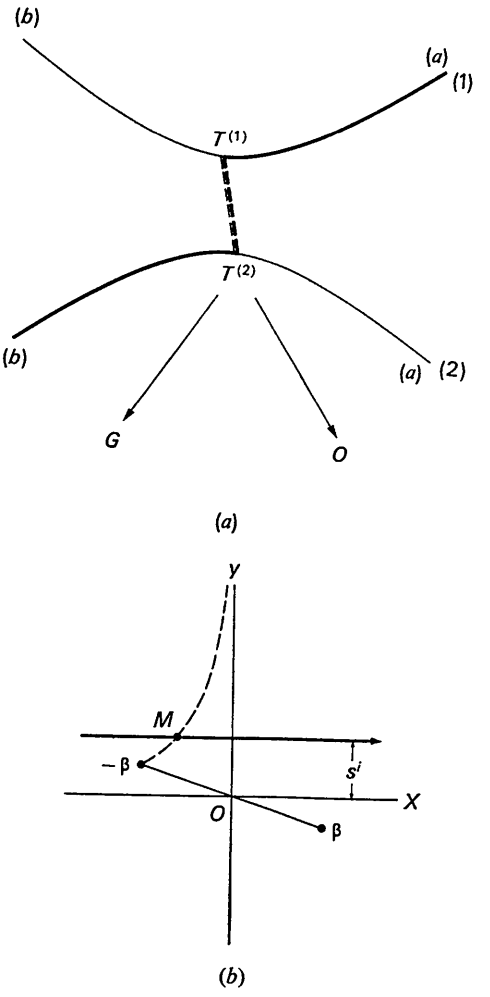

Fig. 3. The specification of a crystal wave by means of (*a*) the dispersion surface and (*b*) the negative Riemann sheet $[-(s^2-\beta^2)^{1/2}]$. The bold lines correspond to each other. $T^{(1)}$ and $T^{(2)}$: The tangential points of the line $\mathbf{n}_e$ to the dispersion surface.

$$\mathbf{k}_0 = \mathbf{K}_e - \left\{-\tfrac{1}{2}\frac{K\chi_0}{\gamma_0} + \alpha(s \pm \sqrt{s^2-\beta^2})\right\}\mathbf{n}_e \quad (2a)$$

$$\mathbf{K}_g = \mathbf{K}_e + \frac{K_x \sin 2\theta_B}{|\gamma_g|}\mathbf{n}_e + 2\pi\mathbf{g}\,. \quad (2b)$$

The factor c is given by the amplitude continuity as

$$c = \left(\frac{\chi_g}{\chi_{-g}}\right)^{1/2}\sqrt{\frac{\gamma_0}{|\gamma_g|}}\,\frac{-s \mp \sqrt{s^2-\beta^2}}{\beta}\,. \quad (3)$$

Here, α and β are defined in the present case as follows

$$\alpha = \frac{\sin 2\theta_B}{2|\gamma_g|} \quad (4a)$$

$$\beta = KC(\chi_g\chi_{-g})^{1/2}\sqrt{\frac{|\gamma_g|}{\gamma_0}}\,\frac{1}{\sin 2\theta_B} \equiv \sqrt{\frac{|\gamma_g|}{\gamma_0}}\,\beta_g\,. \quad (4b)$$

The double signs associated with $\sqrt{s^2-\beta^2}$ correspond to the wings (a) and (b) of the dispersion surface [see Fig. 3(a)].

The solution described above is well known (*e.g.*, Zachariasen, 1945). Here, however, some important properties are summarized for the further development of the theory. The mathematical proofs have been given in a separate paper (Kato, Katagawa & Saka, 1971).

The Poynting vector of the crystal Bloch wave given by equations (1) must satisfy the condition,

$$(\mathbf{s} \cdot \mathbf{n}_e) \geq 0 . \tag{5}$$

This is required by the boundary condition that no wave arrives at the entrance surface from the crystal side. In the Bragg case, unlike the Laue case, only one of the solutions specified by the double signs of $\sqrt{s^2-\beta^2}$ satisfies the requirement (5) for a given incident wave.

In fact, if one considers the quantity $\pm\sqrt{s^2-\beta^2}$ on the positive and negative Riemann sheets of the complex plane, the solution meeting requirement (5) is the one represented* by $-(s^2-\beta^2)^{1/2}$. Also, it has been proved that such a Bloch wave is always attenuated in the crystals. These properties are true irrespective of the magnitude of the absorption and the presence of centrosymmetry. The solution concerned here corresponds to the wings of the dispersion surface which are drawn as bold curves in Fig. 3(a).

In addition, a few significant properties of the plane-wave solution are described by representing the solution on the Riemann sheet. In Fig. 3(b), any mathematical solution can be represented by a single point specified by z. It becomes singular when $z=\pm\beta$. For a given crystal and the geometrical conditions, β^r, β^i and $s^i=\mathrm{Im}(s)$ are fixed. In general, the condition $s^i>|\beta^i|$ is always satisfied owing to the property of the Fourier coefficients, $\chi_0^i>|\chi_g^i|$. For this reason, the physically significant solution is specified by a single point on the bold line in Fig. 3(b), and is no longer singular. This property is important in constructing the spherical-wave solution from the plane-wave solution.

It can be proved that the maximum of the rocking curve is given by the condition

$$s^r s^i = \beta^r \beta^i \tag{6}$$

which is obviously a hyperbola passing through $z=\pm\beta$, the asymptotes being the coordinate axes of the complex plane [see Fig. 3(b)]. The maximum position is simply constructed by taking the intersection M of the line of constant s^i and the hyperbola mentioned above.†

* In this paper, $\omega=(s^2-\beta^2)^{1/2}$ means the solution of $\omega^2=(s^2-\beta^2)$ in which $\mathrm{Re}(\omega)$ is positive for a large value of $\mathrm{Re}(s)\equiv s^r$, whereas $\zeta=\sqrt{s^2-\beta^2}$ is defined always by $\mathrm{Re}(\zeta)\geq 0$ or $\mathrm{Im}(\zeta)\geq 0$ when $\mathrm{Re}(\zeta)=0$.

† Fig. 3(b) is concerned with the case where $\beta^r>0$ and $\beta^i<0$. When $\beta^r\beta^i>0$, one of the points representing $\pm\beta$ and the hyperbola appear in the first quadrant. In any case, the maximum of the rocking curve occurs only at a single value of s^r.

As a preparation to the spherical-wave theory, an alternative expression of the wave fields (1a, b and c) is presented here. By the treatment explained in Appendix B of Part I, the common phase term in equations (1a and b) is reduced to the more convenient form,

$$\{(\mathbf{k}_0-\mathbf{K}_e) \cdot (\mathbf{r}-\mathbf{r}_e)\}+(\mathbf{K}_e \cdot \mathbf{r}) = K_y y + K_z z + \tfrac{1}{2}K\chi_0(l_0+l_g)+\Delta\eta_0 l_0+\Delta\eta_g l_g \tag{7}$$

where the 'Resonanzfehler' $\Delta\eta_0$ and $\Delta\eta_g$ are defined by the same equations (I.15a and b) as in the Laue case, their explicit forms being listed in Table 1, and l_0 and l_g are the coordinates of the observation point P referred to the oblique axes $\hat{\mathbf{K}}_0$ and $\hat{\mathbf{K}}_g$ with the origin at the entrance point E in Fig. 1. By substituting the concrete expressions for the 'Resonanzfehler' into equation (7), the plane-wave solutions can be rewritten in a similar form to equations (I.11a and b) for the Laue case,

$$d_0(\mathbf{r}) = E_e A_0 \exp\{i[-\eta_1(s^2-\beta^2)^{1/2}-\eta_2 s]\} \tag{8a}$$

$$d_g(\mathbf{r}) = E_e A_g \left(\frac{\chi_g}{\chi_{-g}}\right)^{1/2} \sqrt{\frac{\gamma_0}{|\gamma_g|}} \frac{-s+(s^2-\beta^2)^{1/2}}{\beta} \times \exp\{i[-\eta_1(s^2-\beta^2)^{1/2}-\eta_2 s]\} \tag{8b}$$

where, the quantities η_1 and η_2 are linear functions of the position parameters x_0 and t of the observation point P, which are defined in Fig. 1. The explicit expressions of η_1 and η_2 are listed in Table 2. The quantities A_0 and A_g are previously defined by equations (I.13a and b) and the constant phase P involved can be written as $\frac{1}{2}K\chi_0(l_0+l_g)$ also in the present case.

Table 1. *The explicit forms of the Resonanzfehler*

$\Delta\eta_0$	$\gamma_0\alpha\{-s+(s^2-\beta^2)^{1/2}\}$
$\Delta\eta_g$	$\lvert\gamma_g\rvert\alpha\{-s-(s^2-\beta^2)^{1/2}\}$

Table 2. *The explicit forms of η_i and ζ*

η_1	$-\alpha t$
η_2	$x_0+\alpha t$
ζ	$\frac{\gamma_0}{\lvert\gamma_g\rvert} x_g$

The phase term in the vacuum wave (1c) is rewritten in the form, by the use of the relation $\mathbf{r}-\mathbf{r}_e=l_0\hat{\mathbf{K}}_0+l_g\hat{\mathbf{K}}_g$,

$$\frac{K_x \sin 2\theta_B}{|\gamma_g|}((\mathbf{r}-\mathbf{r}_e) \cdot \mathbf{n}_e)+(\mathbf{K}_e \cdot \mathbf{r})+2\pi(\mathbf{g} \cdot \mathbf{r}) = K_y y + K_z z + 2\pi(\mathbf{g} \cdot \mathbf{r}) + P_g - \zeta s \tag{9}$$

where

$$P_g = \tfrac{1}{2}K\chi_0\left(1+\frac{\gamma_0}{|\gamma_g|}\right) l_0 . \tag{10}$$

The analytical expression for position parameter ζ is shown in Table 2. Thus, the wave field (1c) is transformed to

$$E_g(\mathbf{r})=E_eA_{g,r}\left(\frac{\chi_g}{\chi_{-g}}\right)^{1/2}\times\sqrt{\frac{\gamma_0}{|\gamma_g|}}\,\frac{-s+(s^2-\beta^2)^{1/2}}{\beta}\exp(-i\zeta s)\quad(11)$$

where

$$A_{g,r}=\exp i(K_yy+K_zz+2\pi(\mathbf{g}\,.\,\mathbf{r})+P_g)\,.\quad(12)$$

Note that the phase term proportional to $(s^2-\beta^2)^{1/2}$ vanishes in this case.

(*b*) *Spherical-wave theory*

According to the general approach adopted in the present series of papers, the spherical-wave solutions are given by a Fourier transform of the plane-wave solutions (8*a*, *b* and 11). After performing the integration of K_y, the wave fields can be represented in the same form as equations (I.47*a* and *b*);
crystal waves:

$$\phi_0(\mathbf{r})=W_0B_0E_e\quad(13a)$$

$$\phi_g(\mathbf{r})=\left(\frac{\chi_g}{\chi_{-g}}\right)^{1/2}\sqrt{\frac{\gamma_0}{|\gamma_g|}}\,W_gB_gE_e\,.\quad(13b)$$

vacuum wave:

$$\Phi_g(\mathbf{r})=\left(\frac{\chi_g}{\chi_{-g}}\right)^{1/2}\sqrt{\frac{\gamma_0}{|\gamma_g|}}\,W_{g,r}B_{g,r}E_e\quad(13c)$$

where

$$W_0=\int_{-\infty}^{\infty}\exp\{i[-\eta_1(s^2-\beta^2)^{1/2}-\eta_2s]\}\mathrm{d}s^r\quad(14a)$$

$$W_g=\int_{-\infty}^{\infty}\frac{-s+(s^2-\beta^2)^{1/2}}{\beta}\times\exp\{i[-\eta_1(s^2-\beta^2)^{1/2}-\eta_2s\,]\}\,\mathrm{d}s^r\quad(14b)$$

$$W_{g,r}=\int_{-\infty}^{\infty}\frac{-s+(s^2-\beta^2)^{1/2}}{\beta}\exp(-i\zeta s)\mathrm{d}s^r\quad(14c)$$

and

$$B_{g,r}=\frac{i}{8\pi^2}\sqrt{\frac{2\pi}{Kz}}\exp[i(-\frac{\pi}{4}+P_g+Kz+2\pi(\mathbf{g}.\mathbf{r}))].\quad(15)$$

It is significant that only a single Riemann sheet is concerned in the present integral. According to Appendix *A*, the final expressions for the wave fields are given in the forms:

$$\phi_0(\mathbf{r})=-\pi\beta_g\left(\sqrt{\frac{x_g}{x_0}}-\frac{|\gamma_g|}{\gamma_0}\sqrt{\frac{x_0}{x_g}}\right)J_1(\beta_g\sqrt{x_0x_g})\,.\,B_0E_e\quad\text{for } x_0>0$$
$$=0\quad\text{for } x_0<0\quad(16a)$$

$$\phi_g(\mathbf{r})=i\pi\beta_g\left(\frac{\chi_g}{\chi_{-g}}\right)^{1/2}\{J_0(\beta_g\sqrt{x_0x_g})+\frac{|\gamma_g|}{\gamma_0}\frac{x_0}{x_g}J_2(\beta_g\sqrt{x_0x_g})\}\times B_gE_e\text{ for }x_0>0$$
$$=0\quad\text{for } x_0<0\quad(16b)$$

$$\Phi_g(\mathbf{r})=i\pi\beta_g\left(\frac{\chi_g}{\chi_{-g}}\right)^{1/2}\{J_0(\beta_g\sqrt{\gamma_0/|\gamma_g|}\,x_g)+J_2(\beta_g\sqrt{\gamma_0/|\gamma_g|}\,x_g)\}\times B_{g,r}E_e\text{ for }x_g>0$$
$$=0\quad\text{for } x_g<0\,,\quad(16c)$$

where x_0 and x_g are the normal distances from the observation point P to the lines EI and EK respectively in Fig. 1, and J_i are Bessel functions of the ith order. The condition for the wave fields to take an appreciable value is different from that of the Laue case. The wave fields (16*a* and *b*) exist on the left side of the line II' in Fig. 1. We, however, have to be concerned only with the inside of the crystal, namely the triangular region IEC. The solutions in the region $I'EC$ are merely virtual. The argument $\sqrt{x_0x_g}$, therefore, should be regarded as real.

The behaviour of the crystal waves is essentially similar to that of the Laue case. The O wave field, however, is always zero on the entrance surface, where $(x_0/x_g)\,(|\gamma_g|/\gamma_0)=1$ is satisfied. As distinct from the O wave, the G wave is not always zero on the crystal surface, but attenuates rapidly as $J_0+J_2=2J_1(\beta_g\varrho)/(\beta_g\varrho)\sim(\beta_g\varrho)^{-3/2}$ where $\varrho=\sqrt{\gamma_0/|\gamma_g|}\,x_g$. Note, then, that the crystal wave is identical with the vacuum wave on the crystal surface, as should be so from the boundary condition.

The wave field $\Phi_g(\mathbf{r})$ (16*c*) exists on the right side of the line KK'. Again, however, one must be concerned with only the region KEC. The solution on the right side of the crystal surface is a virtual one. Owing to the functional form, the fringe system of the vacuum wave is parallel to the line KK'. The vacuum wave field is essentially the projection of the crystal wave field on the crystal surface along the direction $\bar{\mathbf{K}}_g$. It is worth noting that, unlike the Laue case, all the wave fields (16) depend on the geometrical factor $|\gamma_g|/\gamma_0$.

3. The Bragg–(Bragg)^m case

(*a*) *Plane-wave theory*

When the crystal is terminated by another surface S_a on which the condition of the Bragg case is satisfied, the O wave is partly transmitted into vacuum and the G wave is totally reflected. From the standpoint of the plane-wave considerations, the Bloch wave associated with the dispersion point D in Fig. 2 excites a reflected Bloch wave and a transmitted wave. The dispersion points D_r and T are uniquely determined from the initial one D by the same construction as in the Laue–Bragg case, Type II. The treatment described in Part I, therefore, can be applied to the present (Bragg–Bragg) case.

In the case of weakly absorbing crystals, the reflected Bloch wave arrives at the surface S_e,* and moreover,

* Here, the entrance surface S_e plays the role of the exit surface for the reflected Bloch wave (see the definitions of the entrance and the exit surfaces in Part I). To avoid confusion, S_e and S_a will be called the front and rear surfaces respectively.

multiple reflections at the surfaces S_a and S_e may be expected. The phenomena are denoted by the Bragg–(Bragg)^m cases in the present terminology, and they can be analysed in the same way as the Laue–(Bragg)^m case, Type II. In the following, the equations of Part II are often referred to, but the subscripts must be changed according to Table 3.

Table 3. *The correspondence of the notations in the Laue–(Bragg)^m case, Type* II, *and the Bragg–(Bragg)^m case*

Laue–(Bragg)^m	$\mathbf{r}_e$	$\mathbf{r}_a$	$\mathbf{r}_b$	$\mathbf{n}_e$	$\mathbf{n}_a$	$\mathbf{n}_b$	γ_0'	γ_g'	γ_0''	γ_g''
Bragg–(Bragg)^m	$\mathbf{r}_e$	$\mathbf{r}_e$	$\mathbf{r}_a$	$\mathbf{n}_e$	$-\mathbf{n}_e$	$\mathbf{n}_a$	$-\gamma_0$	$-\gamma_g$	γ_0	γ_g'

$\gamma_0' = (\hat{\mathbf{K}}_0 \cdot \mathbf{n}_a)$ and $\gamma_g' = (\hat{\mathbf{K}}_g \cdot \mathbf{n}_a)$.

In a similar way to equations (II.14*a* and *b*), the boundary conditions are given by,
on the front surface, S_e:

$$0 = d_{0,2n-1} \exp[i(\mathbf{k}_{0,2n-1} \cdot \mathbf{r}_e)] + d_{0,2n} \exp[i(\mathbf{k}_{0,2n} \cdot \mathbf{r}_e)], \quad (17a)$$

on the rear surface, S_a:

$$0 = d_{g,2n} \exp[i(\mathbf{k}_{g,2n} \cdot \mathbf{r}_a)] + d_{g,2n+1} \exp[i(\mathbf{k}_{g,2n+1} \cdot \mathbf{r}_a)], \quad (17b)$$

where the numerical suffixes are defined according to the rule shown in Fig. 4. Combining these with the expression for the amplitude ratio, $d_{g,m}/d_{0,m} = 2\Delta\eta_{0,m}/KC\chi_{-g}$, one can obtain the recurrence formulae for $d_{0,2n}$ and $d_{0,2n+1}$ in terms of the Resonanzfehler as for equation (II.3). Solving the formulae with initial condition (1*a*), one obtains the wave fields in the forms,

$$d_{0,2n}(\mathbf{r}) = \prod_{l=1}^{n} \frac{\Delta\eta_{0,2l-2}}{\Delta\eta_{0,2l-1}} E_e \cdot \exp(i\varphi_{2n}) \exp[i(\mathbf{k}_{0,2n} \cdot \mathbf{r})] \quad (18a)$$

$$d_{0,2n+1}(\mathbf{r}) = -\prod_{l=}^{n+1} \frac{\Delta\eta_{0,2l-2}}{\Delta\eta_{0,2l-1}} E_e \cdot \exp(i\varphi_{2n+1}) \times \exp[i(\mathbf{k}_{0,2n+1} \cdot \mathbf{r})] \quad (18b)$$

$$d_{g,2n}(\mathbf{r}) = \frac{2\Delta\eta_{0,2n}}{KC\chi_{-g}} \prod_{l=1}^{n} \frac{\Delta\eta_{0,2l-2}}{\Delta\eta_{0,2l-1}} E_e \times \exp(i\varphi_{2n}) \exp[i(\mathbf{k}_{g,2n} \cdot \mathbf{r})] \quad (18c)$$

$$d_{g,2n+1}(\mathbf{r}) = -\frac{2\Delta\eta_{0,2n}}{KC\chi_{-g}} \prod_{l=1}^{n} \frac{\Delta\eta_{0,2l-2}}{\Delta\eta_{0,2l-1}} E_e \times \exp(i\varphi_{2n+1}) \exp[i(\mathbf{k}_{g,2n+1} \cdot \mathbf{r})] \quad (18d)$$

where the phases φ_{2n} and φ_{2n+1} have the same expressions as equations (II.17*a* and *b*).

On the other hand, the Resonanzfehler also satisfy recurrence formulae like equations (II.*A*5 and 7). By solving these, one can obtain explicit expressions such as equations (II.*A*8*a*, *b*, *c*, and *d*) in terms of $\Delta\eta_0$ and $\Delta\eta_g$. By using these expressions, equations (18*a*, *b*, *c*, and *d*) can be rewritten in the forms,

$$d_{0,2n}(\mathbf{r}) = \Gamma_{0,n} \frac{\{-s+(s^2-\beta^2)^{1/2}\}^{2n}}{\beta^{2n}} \exp(i\varphi_{2n}) \times \exp[i(\mathbf{k}_{0,2n} \cdot \mathbf{r})] \cdot E_e \quad (19a)$$

$$d_{0,2n+1}(\mathbf{r}) = -\Gamma_{0,n+1} \frac{\{-s+(s^2-\beta^2)^{1/2}\}^{2n+2}}{\beta^{2n+2}} \times \exp(i\varphi_{2n+1}) \exp[i(\mathbf{k}_{0,2n+1} \cdot \mathbf{r})] \cdot E_e \quad (19b)$$

$$d_{g,2n}(\mathbf{r}) = \Gamma_{g,n} \left(\frac{\chi_g}{\chi_{-g}}\right)^{1/2} \sqrt{\frac{\gamma_0}{|\gamma_g|}} \frac{\{-s+(s^2-\beta^2)^{1/2}\}^{2n+1}}{\beta^{2n+1}} \times \exp(i\varphi_{2n}) \exp[i(\mathbf{k}_{g,2n} \cdot \mathbf{r})] \cdot E_e \quad (19c)$$

$$d_{g,2n+1}(\mathbf{r}) = -\Gamma_{g,n} \left(\frac{\chi_g}{\chi_{-g}}\right)^{1/2} \sqrt{\frac{\gamma_0}{|\gamma_g|}} \frac{\{-s+(s^2-\beta^2)^{1/2}\}^{2n+1}}{\beta^{2n+1}} \times \exp(i\varphi_{2n+1}) \exp[i(\mathbf{k}_{g,2n+1} \cdot \mathbf{r})] \cdot E_e \quad (19d)$$

where

$$\Gamma_{0,n} = \left(\frac{\gamma_0}{\gamma_g} \frac{\gamma_g'}{\gamma_0'}\right)^{n^2} \quad (20a)$$

$$\Gamma_{g,n} = \left(\frac{\gamma_0}{\gamma_g} \frac{\gamma_g'}{\gamma_0'}\right)^{n^2+n}. \quad (20b)$$

The phase terms $\varphi_m + (\mathbf{k}_{0,m} \cdot \mathbf{r})$ are expressed in terms of the Resonanzfehler as in the case of the Laue–(Bragg)^m and, therefore, they are rewritten in the form

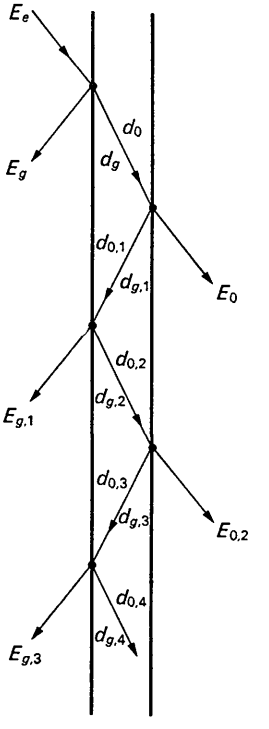

Fig. 4. The specification of the wave fields of the Bragg(Bragg)^m cases in the plane-wave theory.

of $K_y y+K_z z+\frac{1}{2}K\chi_0(l_0+l_g)-\eta_{1,m}(s^2-\beta^2)^{1/2}-\eta_{2,m}s$ (see Appendix *B*). The quantities $\eta_{1,m}$ and $\eta_{2,m}$ are the functions of the position parameters, $x_{0,m}$ and $x_{g,m}$ defined in Fig. 5.

The vacuum wave fields are obtained by similar procedures to those employed in Section 4 of Part II. Writing the *G* and *O* waves, $E_{g,2n+1}(\mathbf{r})$ and $E_{0,2n}(\mathbf{r})$, in the forms $E_{g,2n+1}\exp[i(\mathbf{K}_{g,2n+1}\cdot\mathbf{r})]$ and $E_{0,2n}\exp[i(\mathbf{K}_{0,2n}\cdot\mathbf{r})]$, respectively, one obtains the additional boundary conditions;
on the front surface S_e:

$$E_{g,2n+1}\exp[i(\mathbf{K}_{g,2n+1}\cdot\mathbf{r}_e)] = d_{g,2n+1}\exp[i(\mathbf{k}_{g,2n+1}\cdot\mathbf{r}_e)] + d_{g,2n+2}\exp[i(\mathbf{k}_{g,2n+2}\cdot\mathbf{r}_e)], \quad (21a)$$

on the rear surface S_a:

$$E_{0,2n}\exp[i(\mathbf{K}_{0,2n}\cdot\mathbf{r}_a)] = d_{0,2n}\exp[i(\mathbf{k}_{0,2n}\cdot\mathbf{r}_a)] + d_{0,2n+1}\exp[i(\mathbf{k}_{0,2n+1}\cdot\mathbf{r}_a)]. \quad (21b)$$

From these, the wave fields are given by

$$E_{g,2n+1}(\mathbf{r}) = \{d_{g,2n+1}(\mathbf{r}_e)+d_{g,2n+2}(\mathbf{r}_e)\} \times\exp[i(\mathbf{K}_{g,2n+1}\cdot(\mathbf{r}-\mathbf{r}_e))] \quad (22a)$$

$$E_{0,2n}(\mathbf{r}) = \{d_{0,2n}(\mathbf{r}_a)+d_{0,2n+1}(\mathbf{r}_a)\} \times\exp[i(\mathbf{K}_{0,2n}\cdot(\mathbf{r}-\mathbf{r}_a))]. \quad (22b)$$

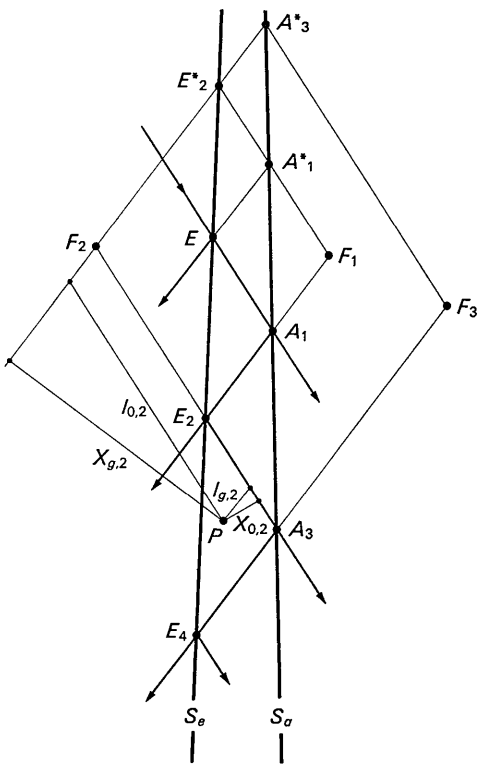

Fig. 5. The Bragg–(Bragg)^m case. F_m is constructed by the same method as in the Laue–(Bragg)^m case. ($l_{0,m}$; $l_{g,m}$) are the coordinates referred to the oblique axes ($\hat{\mathbf{K}}_0$ and $\hat{\mathbf{K}}_g$) with the origin at F_m. ($x_{g,m}$; $x_{0,m}$) = sin $2\theta_B(l_{0,m}; l_{g,m})$, the case for $m=2$ being illustrated.

It is straightforward to represent them in terms of the deviation parameter s as in the case of equations (19) for the crystal waves.

(b) Spherical-wave theory

As in the Bragg case, the spherical-wave solutions of the crystal waves are constructed from the plane-wave solutions (19). The wave fields have the same forms as equations (13). Now, the Fourier integrals similar to W_g *etc.* defined by equations (14) are to be calculated. The details are explained in Appendix *A*. The final expressions are given as follows.

In the region $\eta_1+\eta_2>0$:

$$\phi_{0,2n}(\mathbf{r}) = (i)^{2n}\pi\beta\left\{\left(\frac{\eta_2+\eta_1}{\eta_2-\eta_1}\right)^{n+1/2} J_{2n+1}(\beta\sqrt{\eta_2^2-\eta_1^2}) + \left(\frac{\eta_2+\eta_1}{\eta_2-\eta_1}\right)^{n-1/2} J_{2n-1}(\beta\sqrt{\eta_2^2-\eta_1^2})\right\}\Gamma_{0,n}\cdot B_0E_e \quad (23a)$$

$$\phi_{0,2n+1}(\mathbf{r}) = (i)^{2n}\pi\beta\left\{\left(\frac{\eta_2+\eta_1}{\eta_2-\eta_1}\right)^{n+3/2} J_{2n+3}(\beta\sqrt{\eta_2^2-\eta_1^2}) + \left(\frac{\eta_2+\eta_1}{\eta_2-\eta_1}\right)^{n+1/2} J_{2n+1}(\beta\sqrt{\eta_2^2-\eta_1^2})\right\}\Gamma_{0,n+1}\cdot B_0E_e \quad (23b)$$

$$\phi_{g,2n}(\mathbf{r}) = (i)^{2n+1}\pi\beta_g\left(\frac{\chi_g}{\chi_{-g}}\right)^{1/2} \times\left\{\left(\frac{\eta_2+\eta_1}{\eta_2-\eta_1}\right)^{n+1} J_{2n+2}(\beta\sqrt{\eta_2^2-\eta_1^2}) + \left(\frac{\eta_2+\eta_1}{\eta_2-\eta_1}\right)^{n} J_{2n}(\beta\sqrt{\eta_2^2-\eta_1^2})\right\}\Gamma_{g,n}\cdot B_gE_e \quad (23c)$$

$$\phi_{g,2n+1}(\mathbf{r}) = (i)^{2n+3}\pi\beta_g\left(\frac{\chi_g}{\chi_{-g}}\right)^{1/2} \times\left\{\left(\frac{\eta_2+\eta_1}{\eta_2-\eta_1}\right)^{n+1} J_{2n+2}(\beta\sqrt{\eta_2^2-\eta_1^2}) + \left(\frac{\eta_2+\eta_1}{\eta_2-\eta_1}\right)^{n} J_{2n}(\beta\sqrt{\eta_2^2-\eta_1^2})\right\}\Gamma_{g,n}\cdot B_gE_e. \quad (23d)$$

In the region $\eta_1+\eta_2<0$:

$$\phi_{0,m}(\mathbf{r}) = \phi_{g,m}(\mathbf{r}) = 0 \quad (24)$$

In the expressions (23), η_1 and η_2 are abbreviations for $\eta_{1,m}$ and $\eta_{2,m}$ respectively, and $\Gamma_{0,m}$, $\Gamma_{g,m}$, B_0 and B_g are as previously defined [see equations (20) and (I.48)]. In Table 4, the Bessel functions appearing in the expressions (23) are listed.

Table 4. *Bessel functions appearing in the expressions for the wave fields*

	O		*G*	
Bragg	J_1	J_1	J_0	J_2
Bragg–(Bragg)^{2n}	J_{2n-1}	J_{2n+1}	J_{2n}	J_{2n+2}
Bragg–(Bragg)$^{2n+1}$	J_{2n+1}	J_{2n+3}	J_{2n}	J_{2n+2}

As in the case of Laue–(Bragg)^m, the wave fields (23) are represented in terms of the position parameters $x_{0,m}$ and $x_{g,m}$ by using the expressions of $\eta_{2,m} \pm \eta_{1,m}$ given in Appendix C. In particular, the arguments of the Bessel functions are transformed by

$$\eta_{2,m}^2 - \eta_{1,m}^2 = \frac{\gamma_0}{|\gamma_g|} x_{0,m} x_{g,m} \,. \tag{25}$$

Since $x_{0,m}$ and $x_{g,m}$ are the perpendiculars from the observation point P as defined in Fig. 5, the wave fields show Pendellösung fringes of hyperbolic form, the asymptotes being the lines $\bar{\mathbf{K}}_0$ and $\bar{\mathbf{K}}_g$ passing through a point F_m which is defined in Fig. 5.

The vacuum wave fields are obtained by the Fourier transform of the plane-wave solutions (22*a* and *b*). Obviously, they are the projection of the crystal wave fields on the crystal surfaces S_e or S_a along either one of the directions $\bar{\mathbf{K}}_g$ or $\bar{\mathbf{K}}_0$.

In the case when the crystal is terminated by a surface, the crystal waves may arrive at the surface under the condition of the Laue case. Each of the wave fields of the Bragg–(Bragg)^m–Laue case can be easily obtained by the projection of the crystal wave fields on such a surface along $\bar{\mathbf{K}}_0$ or $\bar{\mathbf{K}}_g$.

4. Discussion

The series of papers (Kato, Katagawa & Saka, 1971; Saka, Katagawa & Kato, 1972*a*, *b*) and the present one treat the wave fields created on the plane surfaces of a perfect crystal. Both plane-wave and spherical-wave theories are developed. The waves are described by successive reflexions and transmission at the surfaces. The diffraction phenomena in more general cases in which the crystal is of finite polyhedral form can be correctly given by a superposition of the wave fields obtained for the cases of Bragg–(Bragg)^m or Laue–(Bragg)^m and Laue (Kato, 1968) as described in the Discussion (*a*) of Part II.

Here, some of the mathematical structures and the physical interpretations of the wave fields are discussed.

(*a*) *Compatibility of the Bragg and Laue–Bragg solutions*

In Part I in which the Laue–Bragg cases were dealt with, it was shown that the crystal wave field of Type I in the region $C\bar{A}J$ of Fig. I.3(*a*) is a superposition of the cylindrical wave emitted from the entrance point E and the reflected one which is a cylindrical wave emitted from an imaginary source F_a. If the entrance point happens to be the edge of the crystal, *i.e.* the intersection of the surfaces S_e and S_a, it is expected that the two cylindrical waves coincide in space. It is interesting to note that the present solution of the Bragg case [*cf.* equations (16*a* and *b*)] is identical to the sum of the wave fields of the Laue and Laue–Bragg cases [*cf.* equations (I.50*a* and *b*)]. Thus, the solution obtained as the Bragg case is compatible with the solution obtained as the Laue and Laue–Bragg cases.

In more general cases when the crystal is terminated by the rear surface, the symbolic relation among the wave fields,

Bragg–(Bragg)^m = (Laue and Laue–Bragg)–(Bragg)^m,

can be seen. Here, the Laue–(Bragg)^m case and Laue–(Bragg)$^{m+1}$ case are obviously of Types II and I respectively. This relation is clear because subsequent reflexions at the rear and front surfaces are irrelevant to how the initial crystal waves are excited. In fact, if one admits this argument, Table 4 of the present paper can be derived directly from Table II.1 without any detailed calculation.

(*b*) *Energy-flow considerations*

The compatibility of the Bragg and Laue–Bragg cases discussed above enables us to interpret correctly the present solution of the Bragg case in terms of energy flow. If one considers hypothetically an X-ray source E_0 inside the crystal, instead of the real entrance point E [see Fig. 6(*a*)], the wave field calculable as the Laue–Bragg case is close to the present solution of the Bragg case provided that E_0 is close to E. Then, the crystal waves can be interpreted in terms of the bundle of rays, one part of which propagates from E_0 directly into the triangular region ME_0I, while the remaining part propagates first into the triangular region KE_0M and is next reflected inside the triangular region $C\bar{A}J$. The vacuum waves are the waves of the latter part transmitted through the crystal surface. If the distance EE_0 is made infinitesimal, the point $\bar{A}$ tends to E and the rays propagating inside the triangular region KE_0M arrive at the point E. They are partly transmitted into vacuum from the point E, and partly reflected and give rise to the crystal wave fields starting from E. Only the rays propagating in the infinitesimally narrow directions parallel to E_0M lead to waves propagating along the crystal surface and the vacuum waves connected

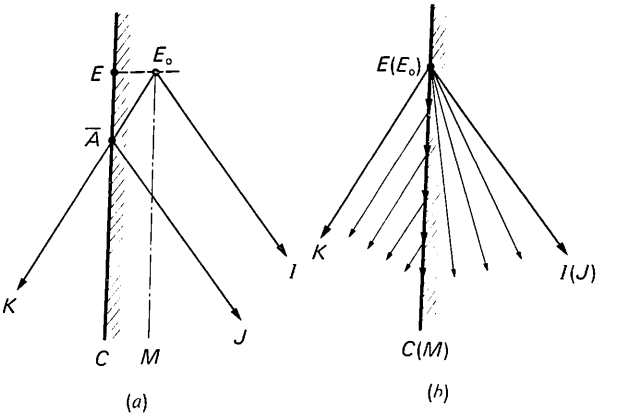

Fig. 6. Interpretation of the energy flow in the Bragg case. (*a*) A hypothetical arrangement. E_0: Hypothetical point source. E: Real entrance point. E_0M is parallel to the crystal surface. (*b*) Real arrangement.

with them. In this way one can obtain a picture of energy flow as described in Fig. 6(*b*).

Incidentally, the imaginary surface denoted by the dotted line in Fig. 6(*a*) for calculating the initial wave field is arbitrary because the wave field of the Laue case is independent of the crystal surface assumed. The hypothetical procedure adopted for initial consideration of the Laue–Bragg case is merely a matter of convention and is equivalent to taking a point source at E_0 inside the crystal.

(*c*) *Comparison with Uragami's results*

The spherical-wave solutions presented in this series of papers are essentially equivalent to the solutions given by Uragami (1969, 1970, 1971) except for a constant factor. The difference can be avoided by taking a correct function as the incident wave in the formulation of dynamical theory by Takagi (1962, 1969) and Taupin (1964).

In the spherical-wave theory, the incident wave is assumed to be $\exp(iKr)/4\pi r$, which is given by the integral expression (I.45). The problem is to find the approximate function for the spherical wave which effectively explains the crystal diffraction at the entrance surface S_e. With the same approximations as those used in the present approach for calculating the crystal wave fields, the spherical wave can be represented on the surface S_e in the form

$$\left[\frac{\exp(iKr)}{4\pi r}\right]_{r=r_e} = \frac{i}{8\pi^2}\sqrt{\frac{2\pi}{Kz}} \times \exp\left[i(-\frac{\pi}{4}+Kz_e)\right]\int_{-\infty}^{+\infty}\exp(iK_x x_e)\mathrm{d}K_x = \frac{i}{4\pi}\sqrt{\frac{2\pi}{Kz}}\exp\left[i(-\frac{\pi}{4}+Kz_e)\right]\delta(x_e) \qquad (26)$$

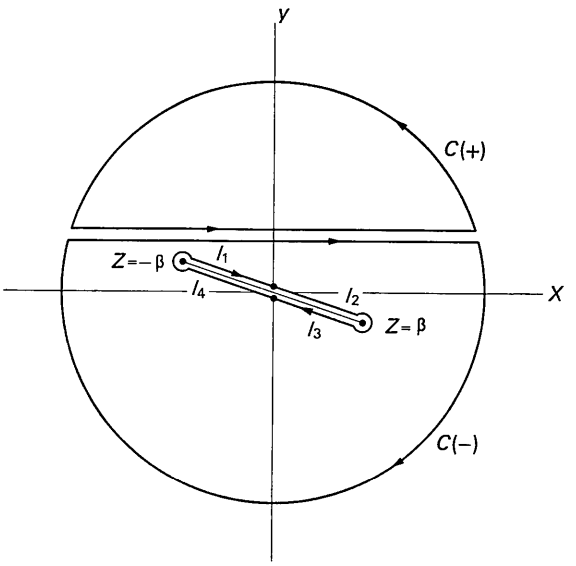

Fig. 7. The path of integration. The contour C is $[l_1+l_2+l_3+l_4]$.

where the suffix e indicates the entrance point. In the Takagi–Taupin approach, therefore, the expression (26) must be used instead of the Dirac delta function $\delta(x)$ as the incident function. In addition, if the phase factor due to the mean wave vector $\bar{\mathbf{k}}_0$, namely

$$\exp[i(\bar{\mathbf{k}}_0 \cdot (\mathbf{r}-\mathbf{r}_e))] = \exp\{i[\tfrac{1}{2}K\chi_0(l_0+l_g)+K(z-z_e)]\} \quad \text{(for the } O \text{ wave)} \qquad (27a)$$

or

$$\exp\{i[2\pi(\mathbf{g}\cdot\mathbf{r}_e)+(\bar{\mathbf{k}}_g\cdot(\mathbf{r}-\mathbf{r}_e))]\} = \exp\{i[2\pi(\mathbf{g}\cdot\mathbf{r})+\tfrac{1}{2}K\chi_0(l_0+l_g)+K(z-z_e)]\} \quad \text{(for the } G \text{ wave)}, \qquad (27b)$$

is multiplied by the solutions obtained by Uragami, it turns out that the final results are identical to the present ones.

The compatibility of the Laue and Laue–Bragg cases is satisfied automatically by taking the present function (26) without the use of the rather arbitrary function in Uragami's approach. The effects of the mean polarizability and absorption can be properly dealt with by taking the factors (27).

APPENDIX *A*
Fourier integrals

In the spherical-wave theory, the following complex integrals are used:

$$W_m = \int_{-\infty+s^l}^{+\infty+s^l} \frac{\{-z+(z^2-\beta^2)^{1/2}\}^m}{\beta^m} \times \exp\{i[-\eta_1(z^2-\beta^2)^{1/2}-\eta_2 z]\}\mathrm{d}z\,. \qquad (A1)$$

The path of integration is shown by the bold line with arrow in Fig. 3(*b*). The integration can be carried out by the standard method of contour integrals. In the present case it is easily shown that

$$\int_{C(-)} I_m(z)\mathrm{d}z = 0 \qquad (\eta_1+\eta_2>0) \quad (A2a)$$

$$\int_{C(+)} I_m(z)\mathrm{d}z = 0 \qquad (\eta_1+\eta_2<0) \quad (A2b)$$

where $I_m(z)$ means the integrand in equation ($A1$) and the contours $C(\pm)$ are the semicircles denoted in Fig. 7. For the case $\eta_1+\eta_2<0$, therefore, W_m is always null. In the other case W_m is given by the integral taken on the path C enclosing two singular points, $z=\pm\beta$. Defining the variable φ by the relations $z=-\beta\sin\varphi$ on l_1 and l_4 and $z=\beta\sin\varphi$ on l_2 and l_3 in Fig. 7, one obtains

$$W_m = \int_C I_m(z)\mathrm{d}z = (i)^m\frac{\beta}{2}\int_0^{2\pi}\{\exp[i(m+1)\varphi]+\exp[i(m-1)\varphi]\} \times \exp[i\beta(-i\eta_1\cos\varphi-\eta_2\sin\varphi)]\mathrm{d}\varphi\,. \qquad (A3)$$

The integral is exactly the same as the integral considered in equation (I.*A*6), so that one can obtain

$$W_m=\pi\beta(i)^m\left[\left(\frac{\eta_2+\eta_1}{\eta_2-\eta_1}\right)^{\frac{m+1}{2}}J_{m+1}(\beta\sqrt{\eta_2^2-\eta_1^2})+\left(\frac{\eta_2+\eta_1}{\eta_2-\eta_1}\right)^{\frac{m+1}{2}}J_{m-1}(\beta\sqrt{\eta_2^2-\eta_1^2})\right]\quad(\eta_1+\eta_2>0)\,. \tag{A4}$$

APPENDIX *B*

The phase terms $\bar{\varphi}_m=\varphi_m+(\mathbf{k}_{0,m}.\mathbf{r})$

By the use of equations (II.17*a* and *b*),† one obtains the recurrence formulae

$$\bar{\varphi}_{2n+1}=\bar{\varphi}_{2n}+\{(\mathbf{k}_{0,2n+1}-\mathbf{k}_{0,2n})\,.\,(\mathbf{r}-\mathbf{r}_a)\} \tag{B1a}$$

$$\bar{\varphi}_{2n}=\bar{\varphi}_{2n-1}+\{(\mathbf{k}_{0,2n}-\mathbf{k}_{0,2n-1})\,.\,(\mathbf{r}-\mathbf{r}_e)\}\,. \tag{B1b}$$

The vectors $\mathbf{r}-\mathbf{r}_a$ and $\mathbf{r}-\mathbf{r}_e$ are represented as follows in terms of coordinates $(l_{0,m};\,l_{g,m})$ with reference to the oblique axes ($\hat{\mathbf{K}}_0$ and $\hat{\mathbf{K}}_g$) with the origin at F_m (*cf.* Fig. 5).

$$\mathbf{r}-\mathbf{r}_a=l_{0,2n+1}\hat{\mathbf{K}}_0+l_{g,2n}\hat{\mathbf{K}}_g\ (\mathbf{r}_a\text{ fixed at }A_{2n+1}) \tag{B2a}$$

$$=l_{0,2n}\hat{\mathbf{K}}_0+l_{g,2n+1}\hat{\mathbf{K}}\ (\mathbf{r}_a\text{ fixed at }A^*_{2n+1}) \tag{B2b}$$

$$\mathbf{r}-\mathbf{r}_e=l_{0,2n-1}\hat{\mathbf{K}}_0+l_{g,2n}\hat{\mathbf{K}}_g\ (\mathbf{r}_e\text{ fixed at }E_{2n}) \tag{B3a}$$

$$=l_{0,2n}\hat{\mathbf{K}}_0+l_{g,2n-1}\hat{\mathbf{K}}_g\ (\mathbf{r}_e\text{ fixed at }E^*_{2n}). \tag{B3b}$$

Since the Resonanzfehler are defined by $\Delta\eta_{0,m}=[\hat{\mathbf{K}}_0\,.\,(\mathbf{k}_m-\bar{\mathbf{k}})]$ and $\Delta\eta_{g,m}=[\hat{\mathbf{K}}_g\,.\,(\mathbf{k}_m-\bar{\mathbf{k}})]$ [see equations (II.*A*2)], the curly brackets in the right of equations (*B*1) are given by the Resonanzfehler. For example, by the use of equation (*B*2*a*), it follows that

$$\{(\mathbf{k}_{0,2n+1}-\mathbf{k}_{0,2n})\,.\,(\mathbf{r}-\mathbf{r}_a)\}=l_{0,2n+1}(\Delta\eta_{0,2n+1}-\Delta\eta_{0,2n})+l_{g,2n}(\Delta\eta_{g,2n+1}-\Delta\eta_{g,2n})\,. \tag{B4}$$

As mentioned in the text each Resonanzfehler is proportional to either $\Delta\eta_0$ or $\Delta\eta_g$, and the phase $\bar{\varphi}_m$ must be given by the form

$$\bar{\varphi}_m=\{K_y y+K_z z+\tfrac{1}{2}K\chi_0(l_0+l_g)\}-\{\eta_{1,m}(s^2-\beta^2)^{1/2}+\eta_{2,m}s\} \tag{B5}$$

where the first term comes from the expression (7) for $\bar{\varphi}_0$ and $\eta_{1,m}$ and $\eta_{2,m}$ are represented by a linear combination of $(x_{0,m};\,x_{g,m})$, *i.e.* $\sin 2\theta_B(l_{g,m};\,l_{0,m})$.

APPENDIX *C*

The expressions for $\eta_{2,m}\pm\eta_{1,m}$

Substituting equations (*B*2*a* and 3*a*) into equations (*B*1*a* and *b*) respectively, and collecting the effective terms for $\eta_{2,m}+\eta_{1,m}$ by means of the operator $[\ ]_+$ defined in the conjunction with equations (I.*B*7), one obtains the relations

$$[\bar{\varphi}_{2n+1}]_+=[\bar{\varphi}_{2n}]_+ +l_{0,2n+1}\Delta\eta_{0,2n+1}-l_{g,2n}\Delta\eta_{g,2n} \tag{C1a}$$

$$[\bar{\varphi}_{2n}]_+=[\bar{\varphi}_{2n-1}]_+ +l_{g,2n}\Delta\eta_{g,2n}-l_{0,2n-1}\Delta\eta_{0,2n-1}\,. \tag{C1b}$$

In deriving these, one uses the relation, $[\Delta\eta_{0,2n}]_+=[\Delta\eta_{g,2n+1}]_+=0$, which follows from the expressions (II.*A*8*a* and *d*).‡ The total sum of these recurrence formulae gives the relations,

$$[\bar{\varphi}_{2n+1}]_+=l_{0,2n+1}\Delta\eta_{0,2n+1} \tag{C2a}$$

$$[\bar{\varphi}_{2n}]_+=l_{g,2n}\Delta\eta_{g,2n}\,. \tag{C2b}$$

Similarly, by the use of equations (*B*2*b* and 3*b*) instead of equations (*B*2*a* and 3*a*), one obtains the relations

$$[\bar{\varphi}_{2n+1}]_-=l_{g,2n+1}\Delta\eta_{g,2n+1} \tag{C3a}$$

$$[\bar{\varphi}_{2n}]_-=l_{0,2n}\Delta\eta_{0,2n} \tag{C3b}$$

for the purpose of calculating $\eta_{2,m}-\eta_{1,m}$. Finally, since every Resonanzfehler is proportional to $\Delta\eta_0$ or $\Delta\eta_g$ [see equations (II.*A*8)], from equations (*C*2 and *C*3) and the expressions in Table 1 for the Resonanzfehler, we obtain the relations,

$$\eta_{2,2n}+\eta_{1,2n}=\left(\frac{\gamma_g}{\gamma_0}\frac{\gamma_0'}{\gamma_g'}\right)^n x_{0,2n} \tag{C4a}$$

$$\eta_{2,2n+1}+\eta_{1,2n+1}=\frac{\gamma_0}{|\gamma_g|}\left(\frac{\gamma_g}{\gamma_0}\frac{\gamma_0'}{\gamma_g'}\right)^{n+1}x_{g,2n+1} \tag{C4b}$$

$$\eta_{2,2n}-\eta_{1,2n}=\frac{\gamma_0}{|\gamma_g|}\left(\frac{\gamma_0}{\gamma_g}\frac{\gamma_g'}{\gamma_0'}\right)^n x_{g,2n} \tag{C4c}$$

$$\eta_{2,2n+1}-\eta_{1,2n+1}=\left(\frac{\gamma_0}{\gamma_g}\frac{\gamma_g'}{\gamma_0'}\right)^{n+1}x_{0,2n+1}\,. \tag{C4d}$$

† Replace the suffixes *a* and *b* by *e* and *a*, respectively.

‡ Replace the factors γ according to Table 3.

References

AFANAS'EV, A. M. & KOHN, V. G. (1971). *Acta Cryst.* A**27**, 421–430.

FINGERLAND, A. (1971). *Acta Cryst.* A**27**, 280–284.

KATO, N. (1968). *J. Appl. Phys.* **39**, 2225–2230.

KATO, N., KATAGAWA, T. & SAKA, T. (1971). *Kristallografiya*, **16**, 1110–1116.

SAKA, T., KATAGAWA, T. & KATO, N. (1972*a*). *Acta Cryst.* A**28**, 102–113.

SAKA, T., KATAGAWA, T. & KATO, N. (1972*b*). *Acta Cryst.* A**28**, 113–120.

TAKAGI, S. (1962). *Acta Cryst.* **15**, 1311–1312.

TAKAGI, S. (1969). *J. Phys. Soc. Japan*, **26**, 1239–1253.

TAUPIN, D. (1964). *Bull. Soc. Fr. Minér. Crist.* **87**, 469–511.

URAGAMI, T. (1969). *J. Phys. Soc. Japan*, **27**, 147–154.

URAGAMI, T. S. (1970). *J. Phys. Soc. Japan*, **28**, 1508–1527.

URAGAMI, T. S. (1971). *J. Phys. Soc. Japan*, **31**, 1141–1161.

WAGNER, H. (1956). *Z. Phys.* **146**, 127–168.

ZACHARIASEN, W. H. (1945). *Theory of X-ray Diffraction in Crystals*. New York: John Wiley.